

1 **Constant Flux Layers with Gravitational Settling: deposition to an**
2 **underlying surface and links to fog.**

3 **Peter A. Taylor**¹

4 6 April 2021

5
6 Received: DD Month YEAR/ Accepted: DD Month YEAR/ Published online: DD Month YEAR

7 © Springer Science + Business Media B. V.

8
9 **Abstract** The turbulent boundary layer concepts of constant flux layers and surface roughness
10 lengths are extended to include gravitational settling and surface deposition of fog or cloud
11 droplets in neutrally and stably stratified atmospheric surface boundary layers.

12
13 **Keywords** Constant flux layers • Fog • Gravitational settling • Surface roughness

14
15 **1. Introduction**

16 Monin-Obukhov Similarity Theory (MOST) considers situations in steady state, horizontally
17 homogeneous, turbulent atmospheric boundary layers where velocity and other variables can be
18 simply dependent on height above the surface, z . In many situations vertical turbulent fluxes of,
19 in particular momentum and heat, can be considered as approximately independent of z . With no
20 sources or sinks of momentum or heat within these constant flux layers one can then use
21 dimensional analysis to predict the form of the profiles. Garratt (1992, section 3.3) or Kaimal and
22 Finnigan (1994) explain Monin-Obukhov similarity while Monin and Obukhov (1954) is a
23 translation of the original Russian work. The simplest case is with neutral stratification where
24 dimensional analysis can be used to infer that the velocity shear, dU/dz is simply proportional to
25 u^*/z where the shear stress, assumed constant with height, is ρu^{*2} , with ρ as air density.

26 Integration of this relationship leads to

27
$$U(z) = (u^*/k) \ln(z/z_{0m}), \tag{1}$$

✉ Peter A. Taylor. pat@yorku.ca

¹ Centre for Research in Earth and Space Science, Lassonde School of Engineering, York University, Toronto, Ontario M3J 1P3, Canada

28 with the roughness length for momentum, z_{0m} , being defined as the height at which a measured
29 profile has $U = 0$ when plotted on a U vs $\ln z$ graph, and where k is the Karman constant with a
30 generally accepted value of 0.4. Noting that z_{0m} values are generally small compared to
31 measurement heights, and after a z_{0m} value has been established for the underlying surface, it is
32 mathematically convenient to modify the relationship to

$$33 \quad U = (u^*/k) \ln((z+z_{0m})/z_{0m}), \quad (2)$$

34 so that we have $U = 0$ on $z = 0$. In eddy viscosity terms this corresponds to

$$35 \quad K_m = ku^*(z+z_{0m}) \quad (3)$$

36 In situations with constant, or near constant fluxes of heat and water vapour, similar
37 logarithmic, or near logarithmic, MOST profiles and eddy diffusivities can be established, based
38 on measured profiles involving z/L where L is the Obukhov length. For potential temperature and
39 water vapour profiles these will involve additional "scalar" roughness lengths, z_{0h} and z_{0v} .
40 Much has been written about roughness lengths and ratios between z_{0m} and z_{0h} , including Chapter
41 5 of Brutsaert (1982). For momentum transfers, form drag on roughness elements, sand grains,
42 blades of grass, bushes, trees, buildings and water waves, can provide most of the drag on the
43 surface and, except over water, z_{0m} is considered as a Reynolds number independent surface
44 property. Water waves are wind speed dependent and z_{0m} needs to take this into account. For heat
45 and water vapour the final transfers from air to the surface involve molecular diffusion and, as a
46 result values of z_{0h} , z_{0v} are significantly lower than z_{0m} . We will introduce a separate roughness
47 length for fog or cloud droplets, z_{0c} . There appears to be very little discussion of a roughness
48 length for cloud droplets in the literature and there is a need for measurements of cloud droplet
49 profiles in fog to establish appropriate values for modelers to work with.

50 Early fog models such as Brown and Roach (1976) or Barker (1977) assume the same
51 eddy diffusivities for water vapour and cloud droplets, presumably with the same roughness
52 lengths while models dealing with deposition of fog water to vegetation, such as Shuttleworth
53 (1977), Lovett (1984) and Katata et al (2008) work in terms of deposition velocity (V_d) and
54 resistance ($1/V_d$) rather than z_{0c} . Over forests, Lovett (1984) points out that there can be
55 "turbulent transfer of cloud droplets to the canopy" and that, in windy conditions "inertial
56 impaction is the dominant mechanism". However, the downward flux of cloud water may be due
57 to both turbulent mixing and gravitational settling, as noted by Katata (2014), although he states

58 that, " For relatively smooth surfaces such as bare soil and water the mechanism of
59 gravitational settling is assumed to be dominant."

60 We consider a situation with fog, or cloud being present and in contact with the lower
61 boundary in, to start with, a neutrally stratified boundary-layer. Our hypothesis is that fog
62 droplets will be deposited at the surface and that this can lead to an approximately constant flux
63 layer situation, if the air in the constant flux layer is at 100% relative humidity. Fog droplets and
64 the associated liquid water mixing ratio will then have a downward flux associated with a
65 combination of gravitational settling of the droplets plus turbulent diffusion and removal due to
66 collision with the surface and coalescence. It is expected that this process will be active over
67 many surfaces and, in particular in marine fog situations over water. It is often claimed that
68 turbulence can enhance the rate of collision and coalescence between droplets in clouds. For
69 example, Franklin (2014) states "Although the effect of turbulence on cloud droplet collision–
70 coalescence rates is yet to be quantified by observations, modelling studies have shown that
71 turbulence can increase the collision rates of droplets by several times the purely gravitational
72 rate." and cites several studies demonstrating this. We anticipate that the same effect will give
73 enhanced deposition of fog droplets to water surfaces.

74

75 **2. A simple model**

76 Based on our hypotheses, we consider an idealized situation where the lowest layers of a
77 horizontally homogeneous boundary-layer fog situation are at 100% relative humidity, are in a
78 steady state and could be considered as having a constant downward flux of uniform size cloud
79 droplets and associated liquid water mixing ratio with a sink at the water surface. The source
80 would be above the constant flux layer where continued cooling of saturated air would create
81 new droplets or allow others to grow. In reality many cloud micro-physics and radiation
82 processes could be involved, but here we consider a simple model with just turbulent transfers
83 and gravitational settling. One could then model the constant downward flux of fog, F_{Qc} , as

$$84 \quad w_s Q_c + k u^*(z + z_{0c}) \frac{dQ_c}{dz} = F_{Qc} = u^* q_c^*, \quad (3)$$

85 where w_s represents the gravitational settling velocity and u^* is the friction velocity. The eddy
86 diffusivity K_{qc} is assumed to be

$$87 \quad K_{qc} = k u^*(z + z_{0c}), \quad (4)$$

88 where z_{0c} is a roughness length for fog droplets with the assumption that $Q_c = Q_{c_{surf}}$ at $z = 0$.

89 Over a water surface we assume $Q_{c_{surf}} = 0$. Initially we can assume a single drop size,
90 with a single w_s and single z_{0c} but, provided we assume that individual drops retain their size and
91 integrity as they pass through the constant flux layer at 100% relative humidity, one can apply
92 these ideas to multiple size bins and combine the profiles of each to get $Q_c(z)$ totals. Assuming
93 constant values for z_{0c} , u^* and w_s one can then solve Eq (3), by integrating factor techniques,
94 multiplying (3) by $(z+z_{0c})^{S-1}/(ku^*)$ where $S = w_s/(ku^*)$, to give,

$$95 \quad (d/dz)[(z+z_{0c})^S Q_c] = (q_c^*/k)(z+z_{0c})^{S-1} \quad (5)$$

96 and, with $Q_c(0) = 0$ the solution is,

$$97 \quad Q_c(z) = (q_c^*/(kS)) [1 - ((z+z_{0c})/z_{0c})^{-S}]. \quad (6)$$

98 In terms of $\zeta = \ln((z+z_{0c})/z_{0c})$, we can write,

$$99 \quad Q_c(\zeta) = (q_c^*/(kS)) [1 - e^{-S\zeta}]. \quad (7)$$

100 These can be referred to as Constant Flux Layer with Gravitational Settling or CFLGS, profiles.

101 In the limit as w_s and $S \rightarrow 0$, as $\zeta \rightarrow 0$, Eq (7) would give $Q_c(\zeta) = (q_c^*/k) \zeta$, a standard log
102 profile.

103

104 3. Some profiles

105 The expected values of w_s and u^* should be considered. Fog droplets have a range of sizes but
106 most fall in the diameter, d , range 0-50 μm , often with bimodal distributions and peaks around 6
107 and 25 μm (see for example Isaac et al, 2020). Applying Stokes law, $w_s = gd^2(\rho_w - \rho)/(18\mu)$, with μ
108 $= \nu\rho_a$, where ν ($15.06 \times 10^{-6} \text{ m}^2 \text{ s}^{-1}$ at 20°C and standard pressure) is the kinematic viscosity of
109 air. With air density, ρ_a (1.178 kg m^{-3}), water droplet density, ρ_w and acceleration due to gravity,
110 g , for these peak sizes we get w_s values of 0.0011 and 0.0192 m s^{-1} . These terminal velocities are
111 clearly small compared to wind speed but for the larger diameter droplets, where the bulk of the
112 liquid water content, $LWC (= \rho_a Q_c)$, is often measured, the terminal velocity corresponds to 69 m
113 per hour and will represent a considerable removal rate in fog which may last several hours or
114 days. The key parameter in our constant flux with gravitational settling model is $S = w_s/ku^*$. In
115 moderate winds over the ocean one might expect u^* values in the 0.2-0.5 m s^{-1} range, while in
116 radiation fog in light winds over land it could be lower. The parameter, S will thus generally be
117 in the range 0.006 to 0.3 over water but could be unlimited in calm conditions over land.

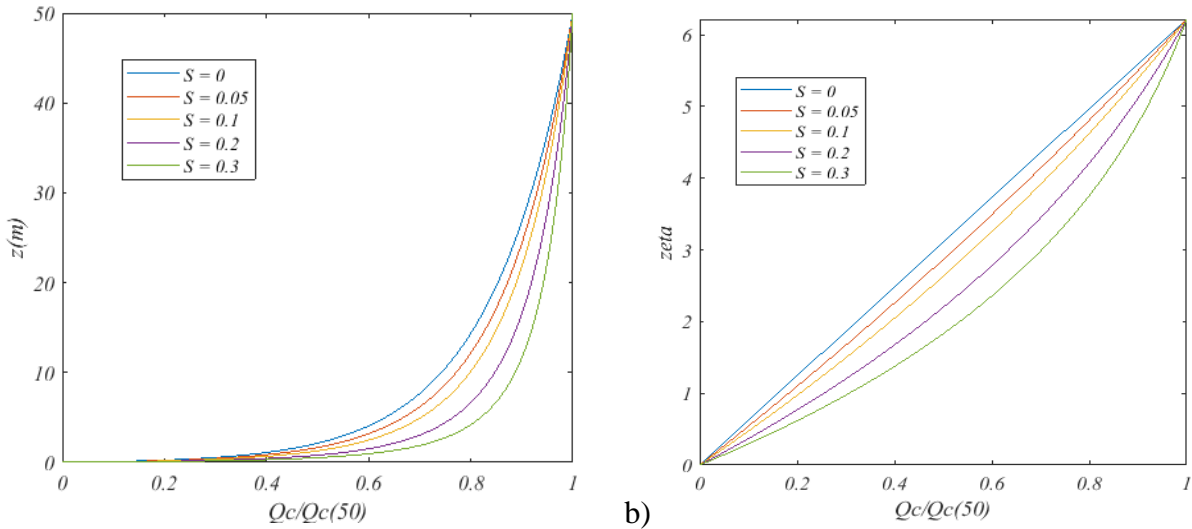
118 At low values of S gravitational settling will have little impact and Q_c profiles will be
 119 approximately logarithmic. To illustrate this Fig. 1 shows Q_c constant flux profiles with linear
 120 and log vertical axes and a range of S values. We have scaled Q_c with a value at 50m. The main
 121 unknown is the value of z_{0c} . Here we use a relatively high value (0.1m) indicating efficient
 122 capture of water droplets by the water surface. Note that these calculations are for uniform sized
 123 droplets, with size related to $w_s^{0.5}$, or $S^{1/2}$ if u^* were fixed. Note that with high S ($= w_s/ku^*$)
 124 values, maybe occurring with low u^* and minimal turbulence, the limiting case would be
 125 constant Q_c down to $z = 0$ and a discontinuity to $Q_c = 0$ at the surface. Calculations with $S = 1$
 126 and 5 (not shown) confirm this. One way to look at the relative importance of gravitational
 127 settling for these uniform size droplets is to consider the relative contributions to the total
 128 downward flux of water droplets ($u^*q_c^*$). The gravitational contribution is simply $w_s Q_c$ while
 129 the turbulent diffusion contribution is,

$$130 \quad ku^*dQ_c/d\zeta = u^*q_c^*e^{-S\zeta}, \text{ where } \zeta = \ln((z+z_{0c})/z_{0c}) \quad (8)$$

131 The ratios of turbulent transfer/total flux and gravitational settling/total flux then become

$$132 \quad TT = e^{-S\zeta} \quad \text{and} \quad GS = 1 - e^{-S\zeta} \quad (9)$$

133



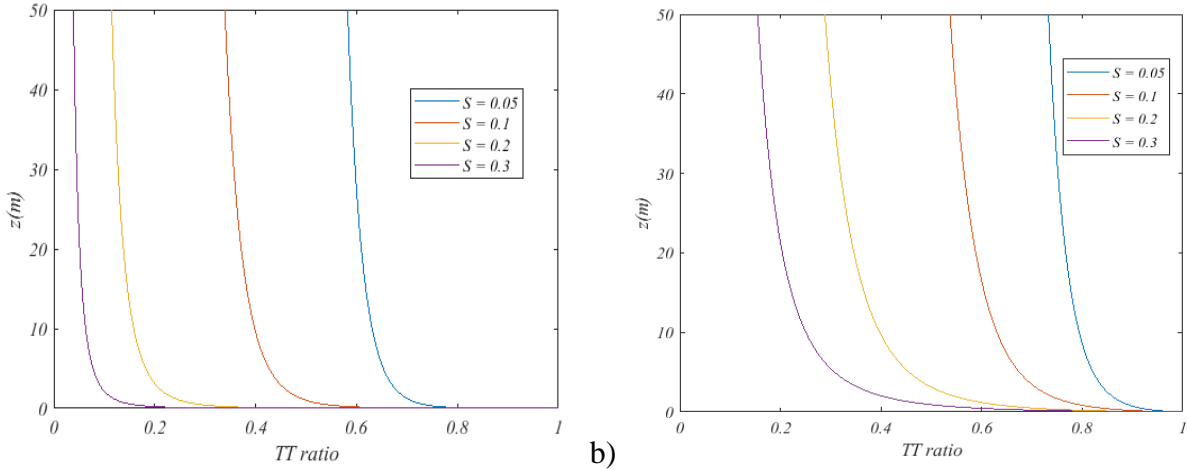
134 a)

b)

135 **Fig. 1** Q_c profiles, scaled by 50 m value, from surface to $z = 50$ m in constant flux layers with
 136 gravitational settling and surface roughness length for water droplet removal, $z_{0c} = 0.1$ m. Linear
 137 (a) and logarithmic (b) height scales.

138

139 Noting that $\zeta = \ln((z+z_{0c})/z_{0c})$ we can see that these ratios depend on both z_{0c} , through the $z(\zeta)$
 140 relationship, and S and will vary with z . Fig. 2 illustrates this. It is important to note that Fig. 2a
 141 is based on a relatively low estimate for z_{0c} , (0.001 m). If we increase it to $z_{0c} = 0.1$ m as in Fig. 1
 142 then turbulent fluxes become more important. We can see that the TT ratio is formally 1 at the
 143 surface, where $Q_c = 0$ so there is no gravitational component. For very large ζ the TT term would
 144 decay to 0 but this would be well above the constant flux layer approximation. At 50 m the value
 145 will depend on S and z_{0c} .
 146



147 a) 148 **Fig. 2** Variation of the Turbulent Transfer fraction of the total Q_c flux and its variation with z
 149 and S . Note that these z values are based on a) $z_{0c} = 0.001$ m and b) $z_{0c} = 0.1$ m
 150
 151

152 4. Stable Stratification Case

153 Over land radiation fog often occurs at low wind speeds with stable stratification. For constant
 154 flux boundary layers in these circumstances MOST has, for velocity, $K_m = k(z+z_{0m})/\Phi_M(z/L)$ and

$$155 \Phi_M(\zeta) = 1 + \beta (z+z_{0m})/L : U = (u^*/k) (\ln((z+z_{0m})/z_{0m}) + \beta z/L). \quad (10)$$

156 Observed profiles give $\beta = 5$ (Garratt 1992, p52). If we extend this idea to $K_{Qc} = k(z+z_{0c})/\Phi_{Qc}(z/L)$
 157 with a similar form for Φ_{Qc} we need to solve,

$$158 w_s Q_c + [ku^*(z+z_{0c})/\Phi_{Qc}(z/L)] dQ_c/dz = F_{Qc} = u^*q_c^*, \text{ or}$$

$$159 dQ_c/dz + S\{(1+\beta(z+z_{0c})/L)/(z+z_{0c})\}Q_c = (q_c^*/k)(1+\beta(z+z_{0c})/L)/(z+z_{0c}); \quad S = w_s/(ku^*)$$

160 The Integrating Factor is $\exp(\int S(1/(z+z_{0c})+\beta/L)dz = (z+z_{0c})^S \exp(S\beta z/L)$ so that

$$161 d [(z+z_{0c})^S \exp(S\beta z/L)Q_c] / dz = (q_c^*/k)(1+\beta(z+z_{0c})/L) (z+z_{0c})^{S-1} \exp(S\beta z/L) \quad (11)$$

162 and we need to integrate the RHS. To do this it is convenient to let $\beta(z+z_{0c})/L = x$ and the integral
 163 that we need is of

164
$$(q_c^*/k)(L/\beta)^{S-1} \exp(-Sx_0) \{(1+x)x^{S-1} \exp(Sx)\} \quad \text{where } x_0 = \beta z_{0c}/L$$

165 After some guidance and a few trials one can see that $d/dx\{x^S \exp(Sx)\} = (Sx^{S-1} + Sx^S) \exp(Sx)$ and
 166 the integral required is simply $F(x,S) = x^S \exp(Sx)/S$. We can then evaluate $F(x,S)$ at $z = 0$, $x_0 =$
 167 $\beta z_{0c}/L$ and any z to allow us to plot Q_c profiles.

168 With stable stratification and light winds the constant flux approximation would only apply to a
 169 relatively shallow layer so we normalize with $Q_c(20m)$ in these cases.

170 Then if $Q_c = 0$ at $z = 0$ we have

171
$$Q_c(z) = [(q_c^*/k)(L/\beta)^{S-1} \exp(-Sx_0) / ((z+z_{0c})^S \exp(S\beta z/L))] [F(x,S) - F(x_0,S)], \quad (12)$$

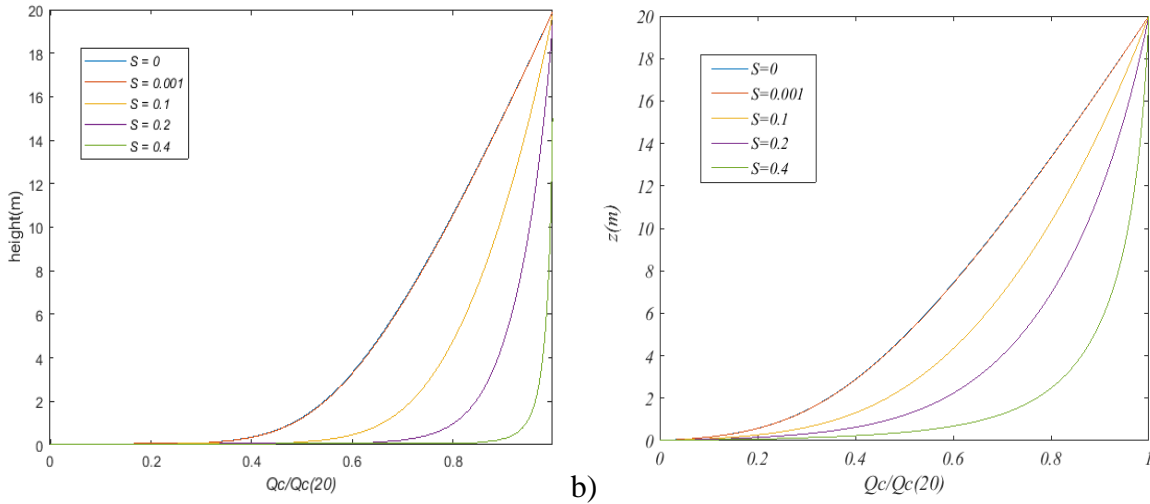
172 where $x = \beta(z+z_{0c})/L$ and $x_0 = \beta z_{0c}/L$ and

173
$$Q_c(z)/Q_c(20) = ((z+z_{0c})^S \exp(S\beta z/L)) [F(x,S) - F(x_0,S)] / \{((20+z_{0c})^S \exp(20S\beta/L)) [F(20,S) - F(x_0,S)]\}$$

174 For $S = 0$, with no gravitational settling, the profile will be essentially the same as the velocity
 175 profile in (A1) above, i.e.

176
$$Q_c(z) = (q_c^*/k) (\ln((z+z_{0c})/z_{0c}) + \beta z/L). \quad (13)$$

177



178 a) b)
 179 **Fig 3.** Profiles with stable stratification, $\Phi_{Q_c}(\zeta) = 1 + \beta(z+z_{0c})/L$, $\beta = 5$, $L = 20m$, $S = 0$ and
 180 0.001 lines overlap as confirmation of our solution form. a) $z_{0c} = 0.001m$, b) $z_{0c} = 0.1m$.

181

182 In addition to z_{0c} and S the key parameter is the Obukhov length, $L = -\rho c_p u_*^3 \theta / (kgH)$, (>0). Neutral
 183 stratification corresponds to $L \rightarrow \infty$ while stable stratification relationships ($H < 0$) are generally

184 limited to $z/L < 1$. If we are concerned with height ranges up to 10 or 20m then $L = 10\text{m}$ would be
185 considered as a very low value maybe with $u^* \approx 0.13 \text{ ms}^{-1}$ and $H \approx -20 \text{ Wm}^{-2}$ as possible values.
186 Figure 3 shows $Q_c(z)/Q_c(20\text{m})$ profiles in a typical case with $z_{0c} = 0.001$ and 0.1m , $L = 20\text{m}$ and
187 a range of S values. For large droplets, $S = 0.4$, Q_c flux is dominated by gravitational settling while
188 for smaller particles, $S = 0, 0.1$ and $z_{0c} = 0.001\text{m}$, turbulent mixing dominates the deposition
189 process.

190

191 **5. Implications and Potential Uses**

192 The basic idea behind this analysis is that, in fog, cloud droplets can both fall toward the
193 underlying surface through gravitational settling and be diffused towards the surface by
194 turbulence. On contact they can coalesce with an underlying water surface or be removed on a
195 hygroscopic surface. Some vegetation surfaces, such as grass, are hydrophobic but we assume
196 that cloud droplets will still be retained and accumulate in drops on the surface so that cloud
197 droplets will still be removed from the air. The modelling assumption used here is that $Q_c(0) = 0$
198 on the surface although bouncing of droplets after impact is a possibility, even on water (Hallett
199 and Christensen 1984). We argue that a water surface can be a significant sink for fog droplets.

200 One can use these ideas in modelling work, adapting the approach of Katata et al (2010,
201 2011) for radiation fog over forests, to deal with marine advection fog over the ocean. A critical
202 unknown parameter in this work is the deposition velocity relating Q_c at the lowest model level
203 to the downward flux to the surface due to turbulent transfer. As in the analysis above, one can
204 use a roughness length for cloud droplets, z_{0c} , as a tuning parameter. Katata et al (2010, 2011)
205 also need a tuning parameter (their "removal efficiency") to establish a relationship between a
206 deposition velocity and the wind speed at some level. The two can be related if there also a
207 known momentum roughness length, z_{0m} , for the surface. Some models treat the diffusion of total
208 water $Q_t = Q_v + Q_c$, where Q_v is water vapour mixing ratio and assume a common roughness
209 length, z_{0q} for Q_t and Q_v . These values are usually very low $\ll z_{0m}$ and based on molecular
210 diffusion of water vapour to or from the surface. The surface boundary condition on Q_t in fog is
211 often based on 100% RH values at the surface implying that $Q_c = 0$ there.

212 The bottom line is that this removal process needs to be taken account of in modelling
213 and forecasting fog occurrence and development and we need to know more about it. Fog is an
214 intermittent phenomenon so setting up 50-m or higher measurement masts in fog-prone locations

215 will be good start. The PARISFOG study (Haeffelin et al 2000) included 30-m masts and
216 LANFEX (Price et al 2018) used 50-m masts but the profile measurements did not include fog
217 water, Q_c , or visibility. In-situ vertical profiles of Q_c were also missing in field programs like
218 FRAM (Gultepe et al 2009) and C-Fog (Fernando et al 2021). C-Fog instrumentation at various
219 sites included 10-m and 15-m masts and also a Radiometrics microwave radiometer for Q_c
220 profile measurements. These may well report interesting measurements but better vertical
221 resolution is desirable. There were Q_c measurements at two or more levels in earlier field
222 measurements reported by Pinnick et al (1978) and Kunkel (1984) showing increases with
223 height. More such measurements are needed with multiple measurement levels and measuring
224 droplet size distributions, Q_c or LWC values and ideally Q_c fluxes, along with wind, turbulence,
225 temperature and humidity profiles plus surface pressure and fluxes of momentum, heat and water
226 vapour. Visibility measurements at multiple levels, 4 component radiation and air, aerosol and
227 fog chemistry measurements could play an important role. From the modelling perspective we
228 need values for z_{0c} , which will depend on surface type and probably on droplet diameter and on
229 wind speed or friction velocity. Assuming that the lower layers, say 10-30 m of a deep fog layer,
230 are in a steady, constant flux layer situation then the CFLGS profiles developed above could
231 provide a framework for analysis of observations.

232 **Acknowledgements** Financial support for this research has come through a Canadian NSERC Collaborative
233 Research and Development grant program (High Resolution Modelling of Weather over the Grand Banks) with
234 Wood Environmental and Infrastructure Solutions as the industrial partner. Discussions with Anton Beljaars, George
235 Isaac and York colleagues over the past year have led me to some of the ideas behind this paper.

236 **References**

- 237 Barker EH (1977) A maritime boundary-layer model for the prediction of fog. *Boundary-Layer Meteorol* 11:267-294
- 238 Brown R, Roach WT (1976) The physics of radiation fog. II. A numerical study *Q. J. R. Meteorol. Soc* 102:335-354
- 239 Brutsaert W (1982) *Evaporation into the Atmosphere*, Reidel, Dordrecht, Holland
- 240 Fernando H, Gultepe I, Dorman C, Pardyjak E, Wang Q, Hoch S, Richter D, Creegan E, Gabersek S, Bullock T, Hocut
241 C, Chang R, Alappattu D, Dimitrova R, Flagg, D, Grachev A, Krishnamurthy R, Singh, D, Lozovatsky I, Fernand
242 H (2021) C-FOG: Life of Coastal Fog. *Bulletin of the American Meteorological Society* 102: 10.1175/BAMS-D-
243 19-0070.1
- 244 Franklin CN (2014) The effects of turbulent collision-coalescence on precipitation formation and precipitation-
245 dynamical feedbacks in simulations of stratocumulus and shallow cumulus convection *Atmos. Chem. Phys* 14:
246 6557-6570
- 247 Garratt JR (1992) *The atmospheric boundary layer*, Cambridge, UK
- 248 Gultepe I, Pearson G, Milbrandt JA, Hansen B, Platnick S, Taylor P, Gordon M, Oakley JP, Cober SG (2009) The

249 Fog Remote Sensing and Modeling (FRAM) field project. *Bull. Amer. Meteor. Soc* 90:341–359

250 Hallett J Christensen L (1984) Splash and penetration of drops in water. *Journal de Recherches Atmospheriques*, 18:
251 225–242.

252 Haeffelin M, Bergot T, Elias T, Tardif R, Carrer D, Chazette P, Colomb M, Drobinski P, Dupont E, Dupont JC (2000)
253 PARISFOG : Shedding new light on fog physical processes. *Bull. Am. Meteorol. Soc* 91:767–783.

254 Isaac GA, Bullock T, Beale J, Beale S (2020) Characterizing and Predicting Marine Fog Offshore Newfoundland and
255 Labrador. *Weather and Forecasting*. 35:347-365

256 Kaimal JC, Finnigan JJ, (1994) *Atmospheric Boundary Layer Flows*, Oxford University Press, UK

257 Katata G, Nagai H, Wrzesinsky T, Klemm O, Eugster W, Burkard R (2008) Development of a land surface model
258 including cloud water deposition on vegetation, *Journal of Applied Meteorology and Climatology*, 47, 2129-2146.

259 Katata G, Nagai H, Kajino M, Ueda H, Hozumi Y (2010), Numerical study of fog deposition on vegetation for
260 atmosphere-land interactions in semi-arid and arid regions, *Agric. For. Meteorol* 150:340–353.

261 Katata G, Kajino M, Hiraki T, Aikawa M, Kobayashi T, Nagai H (2011) A method for simple and accurate estimation
262 of fog deposition in a mountain forest using a meteorological model. *Journal of Geophysical Research*
263 116:D20102.

264 Katata G (2014) Fogwater deposition modeling for terrestrial ecosystems: A review of developments and
265 measurements, *J. Geophys. Res. Atmos* 119: 8137–8159. doi:10.1002/2014JD021669

266 Kunkel A (1984) Parameterization of droplet terminal velocity and extinction coefficient in fog models. *J. Climate*
267 *Appl. Meteor* 23:34–41.

268 Lovett GM (1984) Rates and mechanisms of cloud water deposition to a subalpine balsam fir forest. *Atmos. Environ.*,
269 18: 361–371

270 Monin AS, Obukhov AM (1954) Basic laws of turbulent mixing in the surface layer of the atmosphere, *Contrib.*
271 *Geophys. Inst. Acad. Sci. USSR*, 24 (151):163-187

272 Pinnick R, Hoihjelle DL, Fernandez G, Stenmark EB, Lindberg JD, Hoidale GB, Jennings SG (1978) Vertical structure
273 in atmospheric fog and haze and its effect on visible and infrared extinction. *J. Atmos. Sci* 35:2020–2032.

274 Price JD, Lane S, Boutle IA, Smith DKE, Bergot T, Lac C, Duconge L, McGregor J, Kerr-Munslow A, Pickering M,
275 Clark R (2018) LANFEX: A field and modeling study to improve our understanding and forecasting of radiation
276 fog. *Bull. Amer. Meteor. Soc* 99:2061–2077, <https://doi.org/10.1175/BAMS-D-16-0299.1>.

277 Shuttleworth WJ (1977) The exchange of wind-driven fog and mist between vegetation and the atmosphere.
278 *Boundary-Layer Met* 12:463-489.